

Amplitude zeros in radiative decays of scalar particles

N.G. Deshpande, Xiao-Gang He, and Sechul Oh

Institute of Theoretical Science, University of Oregon, Eugene, Oregon 97403-5203

(Received 27 October 1994)

We study amplitude zeros in radiative decay processes with a photon or a gluon emission of all possible scalar particles (e.g., scalar leptoquarks) which may interact with the usual fermions in models beyond the standard model. For the decays with a photon emission, the amplitudes clearly exhibit the factorization property and the differential decay rates vanish at specific values of a certain variable which are determined only by the electric charges of the particles involved and independent of the particle masses and the various couplings. For the decays with a gluon emission, even though the zeros are washed away, the differential decay rates still have distinct minima. The branching ratios as a function of leptoquark masses are presented for the scalar leptoquark decays. We also comment on the decays of vector particles into two fermions and a photon.

PACS number(s): 13.40.Hq, 12.38.Bx, 12.60.Fr, 14.80.-j

I. INTRODUCTION

It has been known that there is a specific angle at which the angular distribution of the process $q\bar{q} \rightarrow W\gamma$ in lowest order vanishes, the so called radiation amplitude zero (RAZ) phenomenon, if the magnetic moment of the W has the standard model (SM) value $\kappa = 1$ [1]. This phenomenon is a consequence of the factorization property of the four-particle scattering amplitude [2]. For any gauge theory, the internal symmetry (charge) dependence and the polarization (spin) dependence of the scattering amplitude can be factorized into separate parts at the tree level if one or more of the four particles are massless gauge bosons. Such a characteristic phenomenon may provide a test for the magnetic moments of the W [3] and the charge of quarks [4]. The RAZ phenomenon has been studied in a number of processes in the standard model and it has also been investigated for processes with charged Higgs bosons in extensions of the standard model, such as $q\bar{q} \rightarrow H^-\gamma$, $H^\pm \rightarrow q\bar{q}\gamma$ and $H^- \rightarrow \bar{d}\bar{u}\gamma$ (where $\bar{d}\bar{u}$ are squarks with charges $-\frac{1}{3}$ and $-\frac{2}{3}$, respectively) [5-7].

Depending on the particle contents in the model, there are different processes which exhibit RAZ phenomena. The particle contents of the minimal standard $SU(3)_C \times SU(2)_L \times U(1)_Y$ model are (1) gauge particles: a gluon which transforms as **8** under $SU(3)_C$ and does not transform under $SU(2)_L \times U(1)_Y$, W^\pm , Z , and γ which are the gauge particles of $SU(2)_L \times U(1)_Y$; (2) the Higgs particle H which transforms under the SM group as (1, 2, 1); (3) the fermions, which are left-handed quarks Q_L , right-handed up-type quarks u_R and down-type quarks d_R , left-handed leptons L_L , and right-handed charged leptons e_R . Their transformation properties under the SM group are

$$\begin{aligned} Q_L &: (3, 2, \frac{1}{3}); & u_R &: (3, 1, \frac{4}{3}); & d_R &: (3, 1, -\frac{2}{3}); \\ L_L &: (1, 2, -1); & e_R &: (1, 1, -2). \end{aligned} \quad (1)$$

In this model, the factorization property exists in the

processes $q\bar{q} \rightarrow W\gamma$ and $l\bar{\nu} \rightarrow W\gamma$ [8]. If the model is extended to include two or more Higgs doublets, like the supersymmetric SM, charged Higgs particles H^\pm exist. Many theories suggest the existence of new particles. For example, in superstring-inspired E_6 models [9], leptoquarks which couple to a lepton-quark pair naturally appear as the supersymmetric partners of the exotic colored particles which lie in the **27** representation of E_6 . These particles are bosons with fractional charges and color triplets. There are also many particles which can couple to standard fermions directly at the tree level. With new particles there are more processes which exhibit the RAZ phenomenon. It is interesting to study the RAZ phenomenon in all these processes. In Table I, we list all the scalar particles which can couple to the standard fermions at the tree level.

If some of the new particles in Table I are not too heavy, they may be produced in collider experiments. The scalar leptoquark production in hadron colliders or ep colliders has been studied in many papers [10,11]. The discovery limits depend on the strength of the Yukawa couplings λ . For example, it was shown that the discovery limits for pair production of scalar leptoquarks are $M \approx 120$ GeV at the Fermilab Tevatron, and the limits for single production are model dependent [10]. In particular, an ep collider may be considered as an ideal machine to search for leptoquarks. At the DESY ep collider HERA (scalar) leptoquarks with masses as heavy as 200 GeV can be discovered even in the case of couplings as small as 0.01 [11]. Thus, it may be possible, for instance, at HERA, to detect the RAZ phenomenon in the decays of scalar leptoquarks with relatively heavy masses if the couplings are not too small.

In this paper, we study the RAZ phenomena in decay processes with a photon or a gluon emission of all possible scalar particles that can couple to the standard fermions at the tree level. We study these RAZ phenomena in a model independent way. We assume the existence of these particles and find the properties related to the RAZ phenomena. The results can be easily applied to a spe-

TABLE I. Set of scalar multiplets that can couple to the standard model fermions, as well as their quantum numbers under the gauge groups. The fermion bilinears to which the scalars may couple are also shown with the corresponding Yukawa couplings λ . In the table all generation indices are suppressed.

Scalars	Representation		Y	Fermion bilinears
	SU(3)	SU(2)		
H_1	1	2	1	$\lambda_u \bar{Q}_L u_R, \lambda_d \bar{Q}_L d_R,$ $\lambda_e \bar{L}_L e_R$
H_2	8	2	1	$\lambda_2 \bar{Q}_L u_R, \lambda_2 \bar{Q}_L d_R$
H_3	3	2	$\frac{7}{3}$	$\lambda_3 \bar{Q}_L e_R, \lambda_3 \bar{u}_R L_L$
H_4	3	2	$\frac{1}{3}$	$\lambda_4 \bar{d}_R L_L$
H_5	3	1	$-\frac{2}{3}$	$\lambda_5 \bar{Q}_L L_L^c$ $\lambda_5 \bar{u}_R e_R^c$
H_6	3	3	$-\frac{1}{3}$	$\lambda_6 \bar{Q}_L L_L^c$
H_8	3	1	$-\frac{1}{3}$	$\lambda_8 \bar{d}_R e_R^c$
H_9	3	1	$-\frac{2}{3}$	$\lambda_9 \bar{u}_R d_R, \lambda_9 \bar{Q}_L^c Q_L$
H_{10}	$\bar{6}$	1	$-\frac{1}{3}$	$\lambda_{10} \bar{u}_R^c d_R, \lambda_{10} \bar{Q}_L^c Q_L$
H_{11}	3	3	$-\frac{1}{3}$	$\lambda_{11} \bar{Q}_L^c Q_L$
H_{12}	$\bar{6}$	3	$-\frac{1}{3}$	$\lambda_{12} \bar{Q}_L^c Q_L$
H_{13}	3	1	$-\frac{1}{3}$	$\lambda_{13} \bar{u}_R^c u_R$
H_{14}	$\bar{6}$	1	$-\frac{1}{3}$	$\lambda_{14} \bar{u}_R^c u_R$
H_{15}	3	1	$\frac{4}{3}$	$\lambda_{15} \bar{d}_R^c d_R$
H_{16}	$\bar{6}$	1	$\frac{4}{3}$	$\lambda_{16} \bar{d}_R^c d_R$
H_{17}	1	1	-2	$\lambda_{17} \bar{L}_L L_L^c$
H_{18}	1	3	-2	$\lambda_{18} \bar{L}_L L_L^c$
H_{19}	1	1	-4	$\lambda_{19} \bar{e}_R e_R^c$

cific model.

We present in Sec. II the radiative decay cases along with a photon emission and in Sec. III the cases along with a gluon emission. In Sec. IV our conclusions are summarized.

II. CASES WITH THE EMISSION OF A PHOTON

The most general coupling of a scalar S to fermions q_1 and q_2 can be parametrized as

$$\mathcal{L}_{\text{int}} = \bar{q}_1 (A + B\gamma_5) q_2 S, \quad (2)$$

where A and B are model-dependent coupling parameters. To lowest order, there are three diagrams (Fig. 1) which contribute to the radiative decay

$$S(p) \rightarrow q_1(p_1) + \bar{q}_2(p_2) + \gamma(k). \quad (3)$$

The decay amplitude is given by

$$M = M_a + M_b + M_c, \quad (4)$$

where $M_a, M_b,$ and M_c are the amplitudes corresponding to (a), (b), and (c) of Fig. 1, respectively. As mentioned before, there is a factorization property in the decay amplitude M because a massless gauge particle γ appears in the processes. Indeed the decay amplitude can be written in the factorized form as

$$M = ie \left(\frac{Q_S}{p \cdot k} - \frac{Q_1}{p_1 \cdot k} \right) \bar{q}_1(p_1) (A + B\gamma_5) \Pi_\mu q_2(p_2) \epsilon_\gamma^\mu, \quad (5)$$

where Q_S and Q_1 are the electric charges of S and q_1 , respectively, and ϵ_γ^μ is the polarization vector of the photon. Π_μ is defined by

$$\Pi_\mu = \frac{1}{2p_2 \cdot k} [p \cdot k (2p_{1\mu} + \gamma_\mu \gamma \cdot k) - 2p_\mu p_1 \cdot k]. \quad (6)$$

The factor $\left(\frac{Q_S}{p \cdot k} - \frac{Q_1}{p_1 \cdot k} \right)$ causes the RAZ phenomenon and determines the position of the zero.

Here we would like to comment on similar decays of a vector boson into two fermions and a photon. The most general vector boson-fermion coupling can be parametrized as

$$\mathcal{L}_{\text{int}} = \bar{f}_1 \gamma_\mu (a + b\gamma_5) f_2 V^\mu, \quad (7)$$

where a and b are model-dependent coupling parameters. For the decay $V(p) \rightarrow f_1(p_1) \bar{f}_2(p_2) \gamma(k)$, there are three diagrams at the tree level similar to the ones in Fig. 1. The decay amplitude can be written into the factorized form as

$$M = ie \left(\frac{Q_V}{p \cdot k} - \frac{Q_1}{p_1 \cdot k} \right) \bar{f}_1(p_1) \Pi_{\mu\nu} (a + b\gamma_5) f_2(p_2) \epsilon_\gamma^\mu \epsilon_V^\nu, \quad (8)$$

where Q_V and Q_1 are the electric charges of V and f_1 , respectively, and ϵ_γ^μ and ϵ_V^ν are the polarization vectors of the photon and the vector particle, respectively. $\Pi_{\mu\nu}$ is defined by

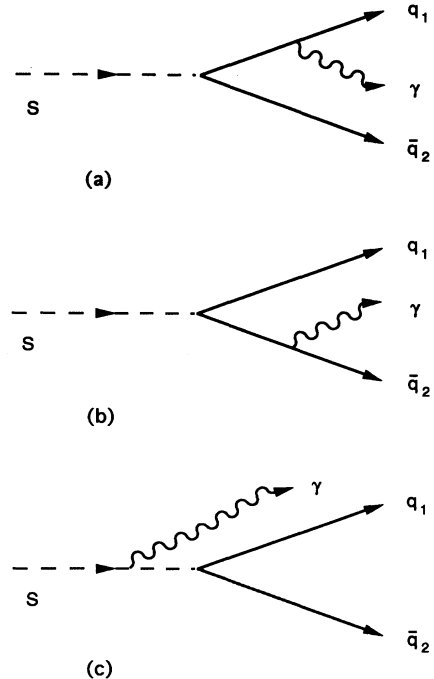


FIG. 1. Tree level diagrams for $S \rightarrow q_1 \bar{q}_2 \gamma$.

$$\Pi_{\mu\nu} = \frac{1}{2p_2 \cdot k} [p \cdot k (2p_{1\mu} + \gamma_\mu \gamma \cdot k) \gamma_\nu - 2p_1 \cdot k (p_\mu \gamma_\nu + \gamma_\mu k_\nu - g_{\mu\nu} \gamma \cdot k)]. \quad (9)$$

We have used the vector-vector-photon vertex which is the same as the W - W -photon vertex, except for the coupling strength given by eQ_V . The factor $(\frac{Q_V}{p \cdot k} - \frac{Q_1}{p_1 \cdot k})$ is the same form as that for the scalar decay given in Eq. (5). We see that the same factorization property exists in vector boson decays.

Table I shows the set of possible scalar multiplets H_1 – H_{19} , as well as their quantum numbers under the gauge groups color $SU(3)_C$, $SU(2)_L$, and hypercharge $U(1)_Y$. We follow the labeling as in Ref. [12]. Since we do not include right-handed neutrinos, H_7 and H_{20} of Ref. [12] are omitted. Also shown in the table is the fermion bilinear products with the corresponding Yukawa couplings.

As a representative example, we consider the scalar leptoquark H_3 in Table I with the Lagrangian

$$\begin{aligned} \mathcal{L}_3 = & \frac{\lambda_3^{ij}}{2} \bar{e}_i (1 - \gamma_5) u_j H_3^{-5/3} + \frac{\lambda_3'^{ij}}{2} \bar{e}_i (1 + \gamma_5) u_j H_3^{-5/3} \\ & + \frac{\lambda_3^{ij}}{2} \bar{e}_i (1 - \gamma_5) d_j H_3^{-2/3} + \frac{\lambda_3'^{ij}}{2} \bar{e}_i (1 + \gamma_5) u_j H_3^{-2/3} \\ & + \text{H.c.}, \end{aligned} \quad (10)$$

where i and j are generation indices, and the Yukawa couplings λ_3^{ij} and $\lambda_3'^{ij}$ are *a priori* arbitrary.

The corresponding decay processes are

$$H_3^{-5/3}(p) \rightarrow e_i(p_1) + \bar{u}_j(p_2) + \gamma(k), \quad (11)$$

$$H_3^{-2/3}(p) \rightarrow e_i(p_1) + \bar{d}_j(p_2) + \gamma(k), \quad (12)$$

and

$$H_3^{-2/3}(p) \rightarrow \nu_i(p_1) + \bar{u}_j(p_2) + \gamma(k), \quad (13)$$

where H , e_i (or ν_i), and \bar{u}_j (or \bar{d}_j) have masses M , m_i , and m_j , and electric charges Q_H , Q_i , and Q_j , respectively. The lowest-order amplitude for $H_3^{-5/3} \rightarrow e_i \bar{u}_j \gamma$ is

$$M_3 = ie \left(\frac{Q_H}{p \cdot k} - \frac{Q_i}{p_1 \cdot k} \right) \bar{e}_i(p_1) (A + B\gamma_5) \Pi_\mu u_j(p_2) \epsilon_\gamma^\mu, \quad (14)$$

where $A = (\lambda_3^{ij} + \lambda_3'^{ij})/2$, $B = (\lambda_3'^{ij} - \lambda_3^{ij})/2$, and Π_μ defined by Eq. (6). The amplitude can be written in a slightly different form as

$$\frac{d^2\Gamma}{dx dy} = \frac{\alpha M}{16\pi^2} Q_H^2 \frac{(y - \bar{Q})^2}{(1 - y^2)} \left\{ (|\lambda_3^{ij}|^2 + |\lambda_3'^{ij}|^2) \left[x + \frac{2(1 - \epsilon)\Omega}{x} \right] + 4(\lambda_3^{ij} \lambda_3'^{ij*} + \lambda_3'^{ij} \lambda_3^{ij*}) \frac{\mu_i \mu_j \Omega}{x} \right\}, \quad (23)$$

with $Q_H = Q_i + Q_j = -5/3$, where

$$\bar{Q} = \frac{Q_i - Q_j}{Q_i + Q_j} \quad (24)$$

$$M_3 = ie \left(\frac{Q_i}{p_1 \cdot k} - \frac{Q_j}{p_2 \cdot k} \right) \bar{e}_i(p_1) (A + B\gamma_5) \Pi'_\mu u_j(p_2) \epsilon_\gamma^\mu, \quad (15)$$

where Π'_μ is defined by

$$\begin{aligned} \Pi'_\mu = & \frac{1}{2p \cdot k} [p_1 \cdot k (2p_{2\mu} + \gamma \cdot k \gamma_\mu) \\ & - p_2 \cdot k (2p_{1\mu} + \gamma_\mu \gamma \cdot k)]. \end{aligned} \quad (16)$$

The amplitudes for $H_3^{-2/3} \rightarrow e_i \bar{d}_j \gamma$ and $H_3^{-2/3} \rightarrow \nu_i \bar{u}_j \gamma$ have the same form as the above one if we put $\lambda_3'^{ij} = 0$ or $\lambda_3^{ij} = 0$, respectively. We see that Eq. (14) is of the general form of Eq. (5). The amplitudes obviously reveal the factorization property and the factor $(\frac{Q_H}{p \cdot k} - \frac{Q_i}{p_1 \cdot k})$ determines the position of the zero in each process.

For convenience, we use the following variables introduced in Ref. [6]:

$$x = \frac{2(p_1 + p_2) \cdot k}{M^2} \quad (17)$$

and

$$y = \frac{(p_1 - p_2) \cdot k}{(p_1 + p_2) \cdot k}. \quad (18)$$

In the H rest frame, x is just the scaled photon energy $2E_\gamma/M$. The x and y limits are given by

$$0 \leq x \leq 1 - r \quad (19)$$

and, for a given fixed x ,

$$\frac{\Delta - \Lambda(x)}{1 - x} \leq y \leq \frac{\Delta + \Lambda(x)}{1 - x}, \quad (20)$$

where

$$\Lambda(x) = \sqrt{(1 - x)^2 - 2(1 - x)\epsilon + \Delta^2}. \quad (21)$$

The parameters r , ϵ , and Δ above are defined as

$$\begin{aligned} \mu_i = & \frac{m_i}{M}, \quad \mu_j = \frac{m_j}{M}, \quad r = (\mu_i + \mu_j)^2, \\ \epsilon = & \mu_i^2 + \mu_j^2, \quad \Delta = \mu_i^2 - \mu_j^2. \end{aligned} \quad (22)$$

The differential decay rate for $H_3^{-5/3} \rightarrow e_i \bar{u}_j \gamma$ in the H rest frame can be described as

and

$$\Omega = 1 - x - 2 \left(\frac{\mu_i^2}{1 + y} + \frac{\mu_j^2}{1 - y} \right). \quad (25)$$

TABLE II. The table shows all possible radiative decays of the scalar particles presented in Table I. The \bar{Q} values for each decay are shown in parentheses.

$H_{1,2}^- \rightarrow \bar{u}_i d_j \gamma$	$(\bar{Q} = \frac{1}{3}),$	$H_1^- \rightarrow e_i \bar{\nu}_j \gamma$	$(\bar{Q} = 1)$
$H_3^{-5/3} \rightarrow e_i \bar{u}_j \gamma$	$(\bar{Q} = 0.2),$	$H_{3,4}^{-2/3} \rightarrow e_i \bar{d}_j \gamma$	$(\bar{Q} = 2)$
$H_3^{-2/3} \rightarrow \nu_i \bar{u}_j \gamma$	$(\bar{Q} = -1),$	$H_4^{1/3} \rightarrow \nu_i \bar{d}_j \gamma$	$(\bar{Q} = -1)$
$H_5^{1/3} \rightarrow \bar{\nu}_i d_j \gamma$	$(\bar{Q} = -1),$	$H_{5,6}^{-1/3} \rightarrow e_i u_j \gamma$	$(\bar{Q} = 5)$
$H_6^{2/3} \rightarrow \nu_i u_j \gamma$	$(\bar{Q} = -1),$	$H_6^{-1/3} \rightarrow \nu_i d_j \gamma$	$(\bar{Q} = -1)$
$H_{6,8}^- \rightarrow e_i d_j \gamma$	$(\bar{Q} = 0.5),$	$H_{9,10,11,12}^{1/3} \rightarrow u_i d_j \gamma$	$(\bar{Q} = 3)$
$H_{9,10,17,18}^- \rightarrow e_i \nu_j \gamma$	$(\bar{Q} = 1),$	$H_{11,12,13,14}^{4/3} \rightarrow u_i u_j \gamma$	$(\bar{Q} = 0)$
$H_{11,12,15,16}^- \rightarrow d_i d_j \gamma$	$(\bar{Q} = 0),$	$H_{18,19}^{-2} \rightarrow e_i e_j \gamma$	$(\bar{Q} = 0)$
$(i, j \text{ generation indices})$			

The differential decay rates for $H_3^{-2/3} \rightarrow e_i \bar{d}_j \gamma$ and $H_3^{-5/3} \rightarrow \nu_i \bar{u}_j \gamma$ have the same form as Eq. (23) with $Q_H = Q_i + Q_j = -2/3$, and $\lambda_3^{ij} = 0$ (for $H_3^{-2/3} \rightarrow e_i \bar{d}_j \gamma$) or $\lambda_3^{ij} = 0$ (for $H_3^{-5/3} \rightarrow \nu_i \bar{u}_j \gamma$). From Eq. (23), it is clear that the differential decay rate vanishes at $y = \bar{Q} = \frac{Q_i - Q_j}{Q_i + Q_j}$ independent of x , the masses, and the couplings. For $H_3^{-5/3} \rightarrow e_i \bar{u}_j \gamma$, $y = \bar{Q} = 0.2$, for $H_3^{-2/3} \rightarrow e_i \bar{d}_j \gamma$, $y = \bar{Q} = 2$, and for $H_3^{-2/3} \rightarrow \nu_i \bar{u}_j \gamma$, $y = \bar{Q} = -1$.

For a fixed x , the y limits are given by Eq. (20). In some decay processes the corresponding values $y = \bar{Q}$ for the RAZ's are not between these limit values and the RAZ's are outside the physical region. Due to this reason, it is impossible to detect the zeros in some of the radiative decays.

We summarize in Table II all possible radiative decay processes together with the corresponding \bar{Q} values. In the table we have omitted processes of the type $H^0 \rightarrow$

$q\bar{q}\gamma$ which does not have a RAZ with finite \bar{Q} . The only detectable RAZ's occur in the radiative decays of $H_1, H_2, H_3, H_6, H_8, H_{11}, H_{12}, H_{13}, H_{14}, H_{18}$, and H_{19} . In some decays, such as $H^- \rightarrow e\bar{\nu}\gamma$, $H^{-2/3} \rightarrow \nu\bar{u}\gamma$ and so on, the RAZ's are just outside the physical region at $y = \bar{Q} = \pm 1$. The general form of the decays showing the detectable zeros is

$$H_\alpha(p) \rightarrow a_i(p_1) + b_j(\text{or } \bar{b}_j)(p_2) + \gamma(k), \quad (26)$$

where a_i and b_j (or \bar{b}_j) denote (anti)lepton or (anti)quark. The indices i and j are generation indices and $\alpha = 1, 2, 3, 6, 8, 11, 12, 13, 14, 18, 19$. The corresponding decay amplitude can be written as

$$M = ie \left(\frac{Q_H}{p \cdot k} - \frac{Q_i}{p_1 \cdot k} \right) \bar{a}_i(p_1) (A + B\gamma_5) \Pi_\mu b_j(p_2) \epsilon_\mu^\nu, \quad (27)$$

where

$$\begin{aligned} A &= B = \frac{\lambda_\alpha^{ij}}{2} \text{ for } H_1, H_2, \text{ and } H_6, \\ A &= -B = \frac{\lambda_\alpha^{ij}}{2} \text{ for } H_8, \\ A &= \frac{1}{2}(\lambda_\alpha^{ij} + \lambda_\alpha^{ij'}) \text{ and } B = \frac{1}{2}(\lambda_\alpha^{ij'} - \lambda_\alpha^{ij}) \text{ for } H_3, H_{11}, H_{12}, H_{13}, H_{14}, H_{18}, H_{19}, \end{aligned}$$

and Π_μ is given by Eq. (6).

In Figs. 2–6, we show some scalar leptoquark decays where the RAZ's are detectable. We normalize the differential decay rate for $H \rightarrow a_i b_j \gamma$ to the corresponding two-body decay rate Γ_0 ($H \rightarrow a_i b_j$). Here Γ_0 is given by

$$\begin{aligned} \Gamma_0 &\equiv \Gamma_0(H \rightarrow a_i b_j) \\ &= \frac{M}{4\pi} \sqrt{1 - 2\epsilon + \Delta^2} [(|\lambda^{ij}|^2 + |\lambda'^{ij}|^2)(1 - \epsilon) + 2(\lambda^{ij} \lambda'^{ij*} + \lambda^{ij*} \lambda'^{ij}) \mu_i \mu_j], \end{aligned} \quad (28)$$

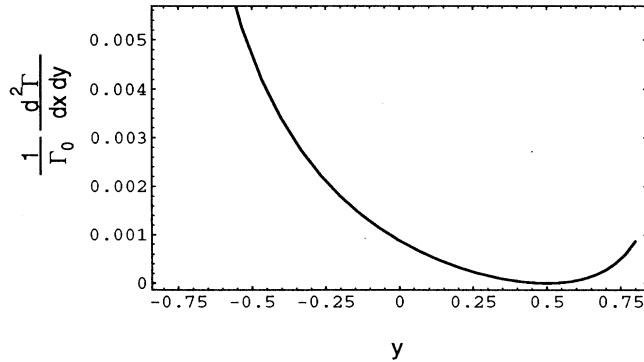


FIG. 2. $(1/\Gamma_0)(d^2\Gamma/dx dy)$ versus y for $H^{-4/3} \rightarrow e b \gamma$ with $x = 0.4$ and $M = 200$ GeV.

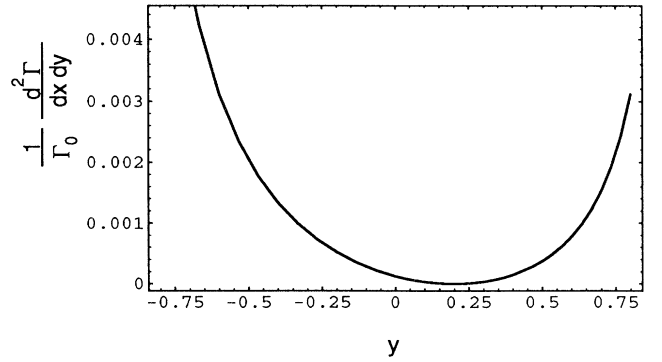


FIG. 3. $(1/\Gamma_0)(d^2\Gamma/dx dy)$ versus y for $H^{-5/3} \rightarrow e \bar{u} \gamma$ with $x = 0.6$ and $M = 150$ GeV ($\lambda_3 = \lambda_3'$).

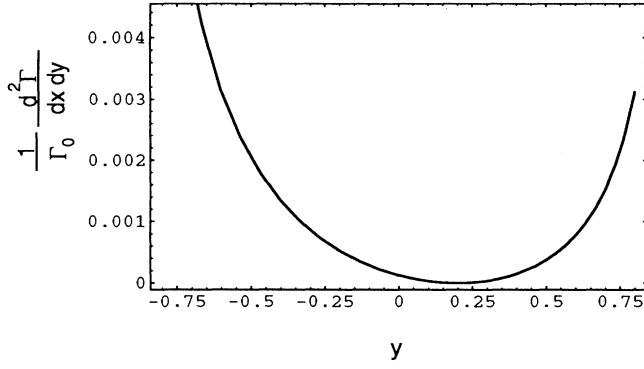


FIG. 4. $(1/\Gamma_0)(d^2\Gamma/dx dy)$ versus y for $H^{-5/3} \rightarrow e\bar{u}\gamma$ with $x = 0.6$ and $M = 150$ GeV ($\lambda_3 = 2\lambda'_3$).

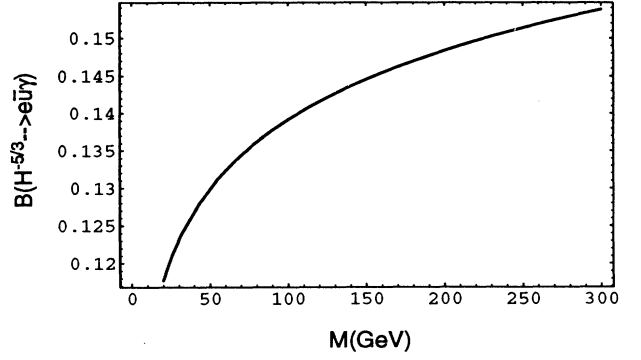


FIG. 6. $B(H^{-5/3} \rightarrow e\bar{u}\gamma)$ versus M with $x \geq 0.1$ and $\lambda_3 = \lambda'_3$.

where we have used the parameters defined by Eq. (22). In the figures we plot $(1/\Gamma_0)(d^2\Gamma/dx dy)$ which shows the position of the RAZ and also indicates the relative branching ratio of the decay $H \rightarrow a_i b_j \gamma$ to that of the decay $H \rightarrow a_i b_j$. In Figs. 2–4, we plot the differential decay rates versus y for the scalar leptoquark decays $H^{-4/3} \rightarrow e b \gamma$ and $H^{-5/3} \rightarrow e \bar{u} \gamma$. Figure 2 shows the result for $H^{-4/3} \rightarrow e b \gamma$ with $x = 0.4$ and $M = 200$ GeV. The plots for $H^{-5/3} \rightarrow e \bar{u} \gamma$ are shown in Fig. 3 with $\lambda_3 = \lambda'_3$, $x = 0.6$, and $M = 150$ GeV, and in Fig. 4 with $\lambda_3 = 2\lambda'_3$, $x = 0.6$, and $M = 150$ GeV. In each case the differential decay rate vanishes at the corresponding values $y = \bar{Q}$ (0.5 and 0.2).

The branching ratios versus M are plotted in Figs. 5 and 6. Figure 5 is for $B(H^{-4/3} \rightarrow e b \gamma) = \Gamma(H^{-4/3} \rightarrow e b \gamma) / \Gamma_0(H^{-4/3} \rightarrow e b)$ and Fig. 6 is for $B(H^{-5/3} \rightarrow e \bar{u} \gamma) = \Gamma(H^{-5/3} \rightarrow e \bar{u} \gamma) / \Gamma_0(H^{-5/3} \rightarrow e \bar{u})$ with $\lambda_3 = \lambda'_3$. In both cases, to ensure identification of photons in the experiment, we have used the cuts on the photon energy: $x \geq x_{\text{cut}} = \frac{2(E_\gamma)_{\text{cut}}}{M} = 0.1$. We see that the ratio of the radiative decays to the two-body decays are reasonably large ($\sim 10\%$). Once these particles are discovered, it is possible to study the RAZ phenomena.

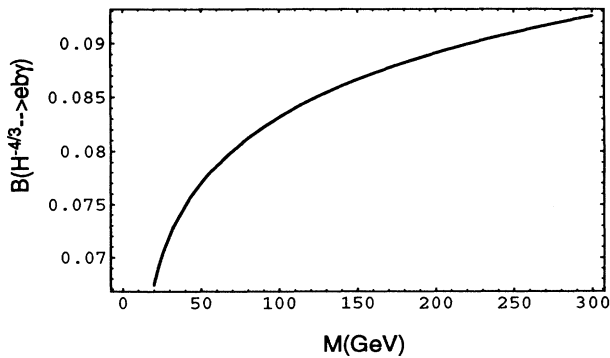


FIG. 5. $B(H^{-4/3} \rightarrow e b \gamma)$ versus M with $x \geq 0.1$.

III. CASES WITH THE EMISSION OF A GLUON

In this section we study the RAZ phenomena in scalar particle decay processes with the emission of a gluon. We shall find in this case that a zero does not appear in the differential decay rate, while the amplitude clearly shows the factorization property and reveals the color charge-dependent factor which is responsible for the zero. The reason is as follows: When we calculate the differential decay rate from the given amplitude, we should sum over all color indices of the final particles, because we cannot detect each color state in experiment. The summation over all color indices of the product particles washes away the zero which at least formally appears in the amplitude.

Now, we investigate this phenomenon specifically. As we can see in Table I, only three types of decay processes may be possible: $SU(3)_C$ triplet, sextet, and octet types.

The Yukawa couplings of the scalar particles to quarks can be written as follows.

$SU(3)_C$ triplet case ($H_3, H_4, H_5, H_6, H_7, H_8, H_9, H_{11}, H_{13}, H_{15}$):

$$\mathcal{L}_{\text{triplet}} = \lambda_t \bar{q}_i^c (1 + \gamma_5) q_j H_k \epsilon^{ijk} + \text{H.c.} \quad (29)$$

$SU(3)_C$ sextet case ($H_{10}, H_{12}, H_{14}, H_{16}$):

$$\mathcal{L}_{\text{sextet}} = \lambda_s \bar{q}_i^c (1 + \gamma_5) q'_j H_{ij} + \text{H.c.} \quad (H_{ij} = -H_{ji}) \quad (30)$$

$SU(3)_C$ octet case (H_2):

$$\mathcal{L}_{\text{octet}} = \lambda_o \bar{q}_i T_{ij}^a (1 + \gamma_5) q'_j H^a + \text{H.c.} \quad (H^{a*} = H^a) \quad (31)$$

Here λ_t , λ_s , and λ_o denote the Yukawa couplings for triplet, sextet, and octet cases, respectively. q and q'

may denote the different quark flavors each other. The indices i, j , and k correspond to the quark color and run from 1 to 3, and a corresponds to the gluon color and runs from 1 to 8. T_{ij}^a is the ij component of $SU(3)_C$ color matrices T^a satisfying

$$[T^a, T^b] = if_{abc}T^c, \quad (32)$$

where f_{abc} are the antisymmetric $SU(3)_C$ structure constants. Here the summation over the repeated indices are assumed.

We consider the three-body decays of the scalar particles defined by Eqs. (29), (30), and (31) into a quark-antiquark pair (or two antiquarks) and a gluon. The Feynman graphs for the triplet case are shown in Fig. 7. For the sextet and the octet cases the Feynman graphs are similar, except that the decaying scalars have different structure of indices such as H_{ij} for the sextet and H^a for the octet.

The amplitudes in each case have the same form except for “the color charge-dependent factor” as follows:

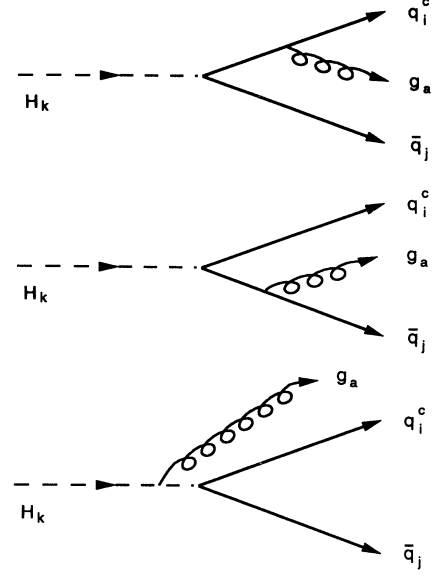


FIG. 7. Tree level diagrams for the triplet case $H_k \rightarrow q_i^c \bar{q}_j g_a$ where g_a denotes a gluon with color index a .

$$M = ig_s \lambda \times (\text{color charge-dependent factor}) \times \bar{q}_i^c(p_1)(1 + \gamma_5)\Pi'_\mu q_j(p_2)\epsilon^{\alpha\mu}, \quad (33)$$

where λ corresponds to λ_t , λ_s , or λ_o in each case and in the octet case $\bar{q}_i^c(p_1)$ is replaced by $\bar{q}_i(p_1)$. $\epsilon^{\alpha\mu}$ is the polarization vector of gluon and Π'_μ is the one defined by Eq. (16). The color charge-dependent factors are given by

$$\left(\text{color charge-dependent factor} \right) = \begin{cases} \sum_m \left(\frac{\epsilon_{im} T_{mj}^a}{p_2 \cdot k} - \frac{\epsilon_{lmj} T_{mi}^a}{p_1 \cdot k} \right) & \text{for the decay of a triplet scalar } H_l, \\ \left(\frac{T_{nj}^a \delta_{mi}}{p_2 \cdot k} - \frac{T_{mi}^a \delta_{nj}}{p_1 \cdot k} \right) & \text{for the decay of a sextet scalar } H_{mn}, \\ \sum_l \left(\frac{T_{il}^b T_{lj}^a}{p_2 \cdot k} + \frac{T_{il}^a T_{lj}^b}{p_1 \cdot k} \right) & \text{for the decay of an octet scalar } H^b. \end{cases} \quad (34)$$

As we have mentioned, the amplitudes clearly reveal the factorization property and the color charge-dependent factors are responsible for the RAZ phenomena. However, to obtain the differential decay rates, we should sum over all color indices of the final particles. For example, in the case of an $SU(3)_C$ triplet scalar decay, the color charge-dependent factor which is now multiplied by the complex conjugate of itself and summed over all color indices gives

$$\begin{aligned} \sum_{ijma} \left| \frac{\epsilon_{im} T_{mj}^a}{p_2 \cdot k} - \frac{\epsilon_{lmj} T_{mi}^a}{p_1 \cdot k} \right|^2 \quad (l \text{ fixed}) &= \frac{8}{3} \left[\frac{1}{(p_1 \cdot k)^2} + \frac{1}{(p_2 \cdot k)^2} + \frac{1}{(p_1 \cdot k)(p_2 \cdot k)} \right] \\ &= \frac{128}{3M^4 x^2} \frac{y^2 + 3}{(1 - y^2)^2}, \end{aligned} \quad (35)$$

where i, j , and m run from 1 to 3 and a runs from 1 to 8, and we have used the variables x and y defined by Eqs. (17) and (18). We note that comparing Eq. (33) with Eq. (15), the differential decay rates obtained from the amplitudes of Eq. (33) have the same form as Eq. (23), except for the color charge-dependent factors multiplied by the complex conjugates of themselves and summed over all color indices, such as Eq. (35). However, since $(y^2 + 3)/(1 - y^2)^2 > 0$, it is obvious that no RAZ phenomena occurs in this case.

The cases of an $SU(3)_C$ sextet and an octet scalar decay show the same phenomena. Explicitly, after being multiplied by the complex conjugates of themselves and summing over all color indices, the color charge-dependent factors give

$$\begin{aligned} \sum_{ija} \left| \frac{T_{nj}^a \delta_{mi}}{p_2 \cdot k} - \frac{T_{mi}^a \delta_{nj}}{p_1 \cdot k} \right|^2 \quad (m, n \text{ fixed}) &= \frac{32}{M^4 x^2} \frac{5y^2 + 3}{(1 - y^2)^2} > 0 & \text{for the sextet case,} \\ \sum_{ijla} \left| \frac{T_{il}^b T_{lj}^a}{p_2 \cdot k} + \frac{T_{il}^a T_{lj}^b}{p_1 \cdot k} \right|^2 \quad (b \text{ fixed}) &= \frac{8}{3M^4 x^2} \frac{9y^2 + 7}{(1 - y^2)^2} > 0 & \text{for the octet case,} \end{aligned} \quad (36)$$

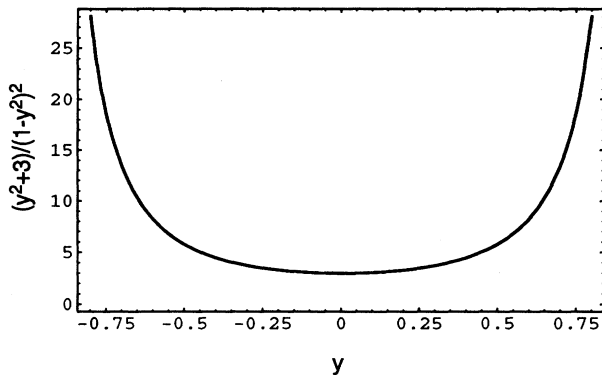


FIG. 8. The plot of $\frac{y^2+3}{(1-y^2)^2}$ versus y . The minimum appears at $y = 0$.

with i, j , and $l = 1, 2, 3$ and $a = 1, 2, \dots, 8$. Figure 8 shows the characteristic curve of the function $(ay^2 + b)/(1 - y^2)^2$ ($a, b > 0$) with $a = 1$ and $b = 3$. The minimum of the function occurs at $y = 0$, independent of a and b .

Therefore, we find that in the cases of the decay along with the emission of a gluon, even though the RAZ's

are washed away, the differential decay rates have the characteristic property—the plot of the differential decay rates versus y behaves like the curve of $(ay^2 + b)/(1 - y^2)^2$ with constants $a, b > 0$ and so has the minimum only at $y = 0$ which is independent of x , the particle masses, and the various couplings.

IV. CONCLUSIONS

We have studied the amplitude zeros in the radiative decay processes (along with the emission of a photon or a gluon) for all possible scalar particles which may interact with the standard fermions at the tree level. For the decays with a photon emission, we have shown that the amplitudes exhibit the expected factorization property and the differential decay rates in the variables x and y vanish at $y = Q$ which is independent of x , the particle masses, and the various couplings λ . The branching ratios versus various leptoquark masses were calculated and plotted for the scalar leptoquark decays.

For the decays with a gluon emission, we have found that even though the RAZ's are washed away, the differential decay rates still have the characteristic property that there is a minimum at $y = 0$ independent of x , the particle masses, and the various couplings.

-
- [1] K.O. Mikaelian, M.A. Samuel, and D. Sahdev, Phys. Rev. Lett. **43**, 746 (1979).
 - [2] Dongpei Zhu, Phys. Rev. D **22**, 2266 (1980); C.J. Goebel, F. Halzen, and J.P. Leveille, *ibid.* **23**, 2682 (1981).
 - [3] J.D. Stroughair and C.L. Bilchak, Z. Phys. C **26**, 415 (1984); G.N. Valenzuela and J. Smith, Phys. Rev. D **31**, 2787 (1985); J. Cortés, K. Hagiwara, and F. Herzog, Nucl. Phys. **B278**, 26 (1986).
 - [4] S. Lakshmibla, Xiao-Gang He, S. Pakvasa, and G. Rajasekaran, Mod. Phys. Lett. A **1**, 277 (1986).
 - [5] Xiao-Gang He and H. Lew, Mod. Phys. Lett. A **3**, 1199 (1988).
 - [6] J. Reid, G. Tupper, G. Li, and M.A. Samuel, Phys. Lett. B **241**, 105 (1990).
 - [7] B. Mukhopadhyaya, M.A. Samuel, J. Reid, and G. Tupper, Phys. Lett. B **247**, 607 (1990).
 - [8] R.W. Brown, D. Sahdev, and K.O. Mikaelian, Phys. Rev. D **20**, 1164 (1979).
 - [9] J.L. Hewett and T.G. Rizzo, Phys. Rep. **183**, 193 (1989).
 - [10] J.L. Hewett and S. Pakvasa, Phys. Rev. D **37**, 3165 (1988); M. de Montigny and L. Marleau, *ibid.* **40**, 2869 (1989).
 - [11] W. Buchmüller, R. Rückl, and D. Wyler, Phys. Lett. B **191**, 442 (1987); A. Dobado, M.J. Herrero, and C. Muñoz, *ibid.* **191**, 449 (1987).
 - [12] A.J. Davies and Xiao-Gang He, Phys. Rev. D **43**, 225 (1991).